International Journal of ChemTech Research
CODEN(USA): IJCRGG ISSN : 0974-4290
Vol.2, No.3, pp 1445-1453, July-Sept 2010

Linear And Nonlinear Optical Properties Of NLO Active L-Phenylalanine L-Phenylalaninium Nitrate Single Crystals

A. Cyrac Peter[1*], M. Vimalan[2], P. Sagayaraj[3], T.Rajesh Kumar[3] and J. Madhavan[3]

[1]Thirumalai Engineering College, Kanchipuram-631551, India.

Tel: 044-27277866.

[2]S.T.Hindu College, Nagercoil-629002, India.

[3]Department of Physics, Loyola College, Chennai-600034, India.

[*]*Corres.author: cyrac.peter@gmail.com*

Abstract: The organic non-linear optical crystal L-phenylalanine L-phenylalaninium nitrate (LPAN) was grown by slow evaporation technique using water as solvent has been synthesized. The solubility studies have been carried out in the temperature range 30–50˚C. Single crystals (15 x 4 x 3 mm^3) have been grown by slow evaporation of the saturated aqueous solution at 30 ◦C. The lattice parameters of the grown crystals have been determined by single crystal X-ray diffraction technique. The UV–vis–NIR absorption spectrum has been recorded in the range 200–2000 nm. The molecular structure was confirmed by FT-IR. LPAN was thermally stable up to 168°C as determined by TG/DTA curves. By a modified Kurtz and Perry method, the powder SHG efficiency was found to be 1.7 times that of KDP. Laser damage threshold of LPAN was determined using a Nd:YAG laser (1064 nm). Dielectric constant and dielectric loss of LPAN are measured in the range from 50 Hz to 5 MHz at different temperatures. Photoconductivity studies of LPAN crystals revealed the negative photoconducting nature.

Keywords: Solubility; Solution growth; Single crystals; Nonlinear optical material.

1. Introduction

Phenylalanine is one of the twenty biologically naturally occurring amino acids that can be found in protein. It contains an amino group, a phenyl ring and a carboxylic group. It is an essential amino acid. The primary dietary sources of phenylalanine are high protein foods such as meat, fish, eggs and dairy products[1] L –phenylalanine is used by the body to build neurotransmitters, chemicals which conduct electrical impulses in the brain and nervous system[2].The biological importance and supermolecular properties of these molecules has motivated us to a number of characteristic studies on these species. A thorough scan of literature reveals that several spectroscopic studies on the behavior of many amino acids and peptides including phenylalanine and on complexes involving amino acids, organic molecules and metal ions[3–7].

L-phenylalanine hydrochloride[8], bis (L-phenylalanine) sulfatemonohydrate[9], and L-Phenylalanine L-phenylalaninium perchlorate[10], crystal structure have been reported As a follow up, the new class of L-phenylalanine compounds with nitric acid composition by successfully crystallizing the crystals of L-phenylalanine L-phenylalaninium nitrate (LPAN)[11]. Both phenylalanine residues have similar geometries in both residues, the bond distances C-O and C=O are nearly equal and the single-bonded O atoms. This may refer to a short hydrogen bond between the singly bonded carboxyl O atoms, as found in L-Phenylalanine L-phenylalaninium perchlorate However, this H atom could not be located unequivocally. Hence, taking into account the equality of the C-O distances, it can be surmised that the two residues may be connected by either a symmetric hydrogen bond with the H atom disordered over two positions. In the present study, bulk single crystals of LPAN with molecular formula $C_9H_{11}NO_2 .C_9H_{12}NO_2^+.NO_3^-$ were grown and the optimized growth conditions are reported. A thorough scan on literature reveals that only the structure of LPAN has been solved by Srinivasan et al .using tiny crystals and no other systematic study has been made on this crystal. Hence, attempts are made to grow bulk crystals of LPAN and characterize the grown crystals by single crystal X-ray diffraction (XRD), Fourier transform infra-red (FT-IR), UV-Vis-NIR, TG/DTA, microhardness, dielectric and photoconductivity, ac/dc conductivity studies. The SHG efficiency and damage threshold of the LPAN were also studied using Nd : YAG Q-switched laser.

2. Experimental

2.1. Synthesis

The starting material was synthesized by taking L-phenylalanine and nitric acid in a 2:1 stoichiometric ratio. The required amount of starting materials for the synthesis of L-phenylalanine L-phenylalaninium nitrate (LPAN) salt was calculated according to the following reaction:

$$2(C_9H_{11}NO_2) + HNO_3 \longrightarrow C_9H_{11}NO_2 .C_9H_{12}NO_2^+ .NO_3^-$$

The calculated amount of nitric acid was first dissolved in deionized water. L-phenylalanine was then added to the solution slowly by stirring. The prepared solution was allowed to dry at room temperature and the salts were obtained by slow evaporation technique. The purity of the synthesized salt was further improved by successive recrystallization process.

2.2. Solubility of LPAN

In solution growth techniques, the size of a crystal depends on the amount of the material available in the solution which in turn is decided by the solubility of the material in the solvent. The solubility of LPAN in deionized water was determined as a function of temperature in the temperature range of 30–50°C. The beaker containing the solution was maintained at a constant temperature and continuously stirred. The amount of LPAN required to saturate at this temperature was estimated and this process repeated for various temperatures. On reaching saturation, the equilibrium concentration of the solute was determined by gravimetric method. The variation of solubility with temperature is shown in Fig.1.

2.3. Growth of LPAN

Single crystals of LPAN were grown by slow solvent evaporation technique at room temperature. Saturated solution was prepared according to the solubility data (Fig. 1), using the recrystallized salt of LPAN. The solution was stirred for one day using magnetic stirrer and then filtered using filter paper. Seed crystals were formed due to spontaneous nucleation in a period of 4-6 days, colorless, transparent, and defect free crystals with perfect, shapes were chosen as seeds to carryout the further growth experiments. The seeds were seasoned and then hung in the beaker containing the supersaturated solution, using a nylon thread and the growth was achieved by slow solvent evaporation technique at a constant temperature of 30°C Good optical quality and well defined single crystals of dimension up to 15 x 4 x 3 mm^3 were grown in a period of 35-40 days. Fig. 2. shows the photograph of as grown single crystals of LPAN.

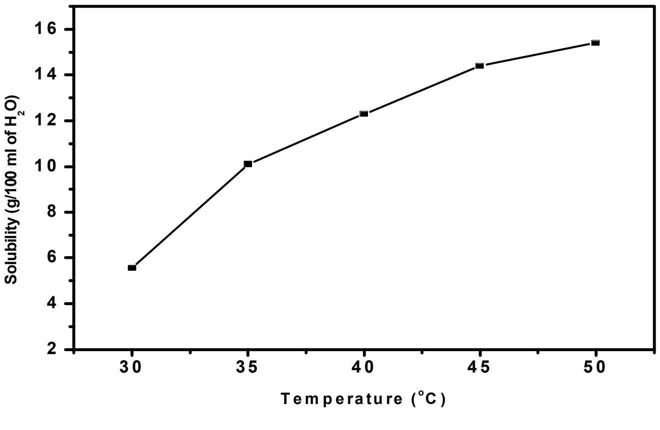

Fig.1. Solubility curve of LPAN

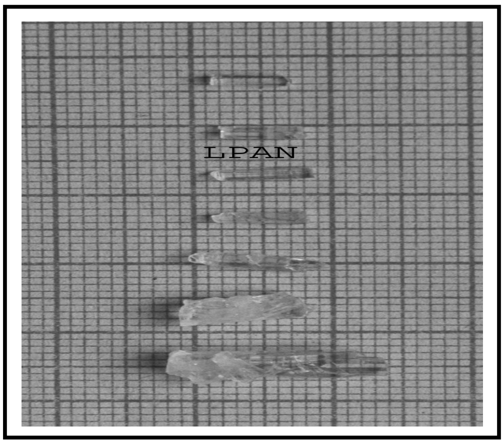

Fig.2. Photograph of as grown LPAN single crystal

2.4. Characterization

The single crystal XRD was collected using an automated diffractometer (MESSRS ENRAF NONIUS CAD4-F, The Netherlands). The structure was solved by the direct method and refined by the full matrix least square technique using the SHELXL program. The Fourier transform infrared analysis was carried out between 400 and 4000 cm^{-1} by recording the spectrum using BRUKER IFS 66V FT-IR SPECTROMETER. The UV-Vis-NIR spectrum was recorded in the range of 200 - 2000nm using VARIAN CARY 5E model spectrophotometer. The NLO efficiency of LPAN crystal was evaluated by Kurtz and Perry powder technique (Kurtz and Perry 1968) using a Q-switched, mode locked Nd : YAG laser emitting 1.064 µm, 8 ns laser pulses with spot radius of 1 mm. The input laser beam was passed through an IR reflector and then directed on the powdered sample. The light emitted by the sample was measured by the photodiode detector and oscilloscope assembly. The TGA and DTA analysis of LPAN were carried between 46 and 485°C at a heating rate of 10°C / min using the instrument NETZSCH STA 409C. Microhardness studies have been carried out on LPAN crystal using a Leitz Wetzlar Vickers microhardness tester fitted with a Vickers diamond pyramidal indenter attached to an incident light microscope. The static indentations were made at room temperature with a constant indentation time of 10 seconds for all indentations. The indentation marks were made on the surfaces by varying the load from 10 to 50g. As microcracks were observed at higher loads, the maximum applied load was restricted upto 50g only. The *ac* conductivity, dielectric constant and dielectric loss of the LPAN sample were studied at room temperature using HIOKI 3532-50 LCR HITESTER in the frequency range 50 Hz to 5 MHz. LPAN sample of uniform cross sectional area 2 x 2 mm^2 and thickness 1 mm was coated with silver paint to provide good ohmic contact. The dielectric constant and dielectric loss were measured by varying the frequency, for a fixed applied voltage. The measurements of *dc* electrical conductivity were done using the conventional two-probe technique for temperatures ranging from 313 to 423 K. The photocurrent and darkcurrent of the crystal was measured using Keithley 485 picoammeter. The experiment was performed at room temperature.

3. Results and discussion

3.1. Single crystal XRD Study

The single crystal X-ray diffraction has been carried out using Enraf Nonius-CAD4 diffractometer. From the measurements we found that the grown specimen of LPAN belongs to monoclinic with a non-centro symmetric space group $P2_1$, with the lattice parameters a = 12.530 Å, b = 5.375 Å, c = 14.96 Å and cell volume V =959.89Å^3. The values reveal a very close agreement with the reported values [11].

3.2. FT-IR Analysis

FT-IR spectrum was of LPAN recorded in the range of 400–4000 cm^{-1} .The spectrum (Fig. 3) shows the presence of all the functional groups in LPAN crystal and is summarized in Table.1. The broad envelope between 300 and 2300 cm^{-1} includes absorption of stretching bands due to NH_3^+ ion of the amino acid. This region results from superimposed O–H and NH_3^+ stretching bands. Strong carbonyl absorption at 1722.30 cm^{-1} identifies the COOH and COO^- groups of the compound. Multiple fine structures at the lower energy mode of the envelope indicates the strong hydrogen bonding interaction of NH_3^+ group with weak absorptions of COO^- group at 1596.10 cm^{-1}. The NO_3^- vibrations produce characteristic peaks at 1382.84 cm^{-1}, 1090.1 cm^{-1} and 855.66 cm^{-1}. These vibrations clearly demonstrate the existence of L-phenylalanine in its salt form with nitric acid. The

NH_3^+ symmetric vibration produce peak at 1498 cm^{-1}. Further strong band observed at about 1213.02 cm^{-1} is due to C-COO^- stretching. The C-O stretching mode is observed at 1108 cm^{-1}, the C-CN scissoring (855.66 cm^{-1})and COO^-wagging (660 cm^{-1}).

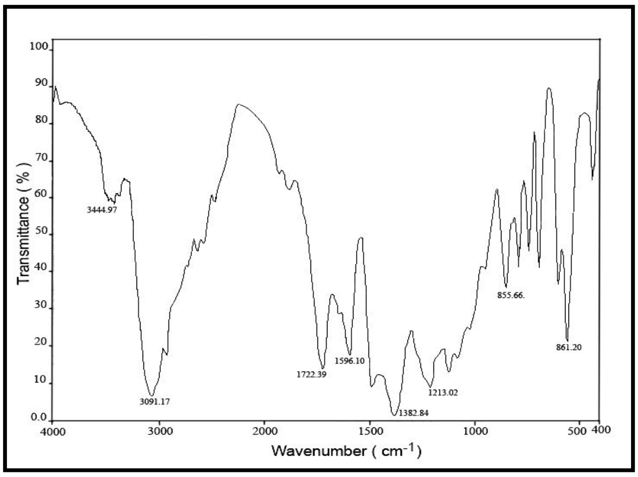

Fig. 3. FT-IR spectrum of LPAN

Table.1. FT-IR frequency assignment for LPAN

Wave number (cm^{-1})	**Assignment**
3444.97	O-H stretch of COOH
3091.17	NH_3^+ asymmetric vibration
2955	CH vibration
2592	NH_3^+ symmetric vibration
1722	C = O stretching vibrations
1624	asymmetrical NH_3^+ bending vibration
1596.10	COO^- asymmetric stretching
1498	NH_3^+ symmetric vibration
1382.84	asymmetric stretching of NO_3^-
1213.02	C- COO^- stretching
1090	symmetric stretching of NO_3^-
855.66	C-CN scissoring
699.54	–COO bend

3.3. UV-Vis-NIR spectral analysis

The UV-Vis-NIR spectrum gives information about the structure of molecule because the absorption of UV and visible light involves the promotion of the electrons in the σ and π orbitals from the ground state to higher energy states. The absorption spectrum is shown in Fig. 4. absorption spectral analysis is important for any NLO material because a NLO can be of practical use only if it has wide transparency window. From the spectra, it is evident that LPAN crystal has UV cut-off around 300 nm and it can be seen from the absorbance curve that LPAN is absorption from 300 to 1500 nm, which is sufficiently low for SHG laser radiation at 1064 nm or other applications in the blue region.

3.4. NLO Properties

The most widely used technique for confirming the SHG from prospective second–order NLO material is the Kurtz powder technique. In addition to identifying the materials with noncentro-symmetric crystal structure, it is also used as a screening technique to identify the materials with the capacity for phase matching. The fundamental beam of 1064 nm with 8ns pulse width from Q-swithed Nd:YAG laser is used as the source and directed on the powdered sample through a visible blocking filter. The doubling of frequency was confirmed by the emission of green radiation of wavelength 532nm collected by a monochromator after separating the 1064 nm pump beam with an IF blocking filter. The powdered samples were tightly packed in the separate microcapillary tubes of uniform diameter (0.154mm).The input laser energy incident on the capillary tube was chosen as 6 mJ. The SHG was confirmed by the emission of green radiation (532nm) and the optical signal was collected by a photomultiplier tube (PMT).The optical signal incident on PMT was converted into voltage output at the CRO. The second harmonic signal of 93 mV was obtained for LPAN with reference to KDP (55 mV). The LPAN shows a powder SHG efficiency of 1.7 times that of standard NLO material, KDP.

3.5. Laser damage threshold

Laser damage studies on NLO crystals are extremely important as the surface damage of the crystal by high power laser limits its performance in NLO application. One of the criteria for a NLO crystal to perform as a device is its resistance to laser damage, since high optical intensities are involved in nonlinear processes. If the material has a low damage threshold, it severely limits its application, though it may have excellent properties like high optical transmittance and high SHG efficiency[12].In the present study, an actively Q-switched diode array side pumped Nd:YAG laser is used for the laser induced damaged threshold studies. A well polished sample with clean surface was taken for this present study. The damage was observed and the energy of the laser beam was measured by power meter. The laser damage threshold value was calculated from this laser energy divided by the focused beam area. The laser damage energy density was found to be 7.8 GW/cm^2. The subject of material damage is of great importance to the design and successful operation of nonlinear devices.

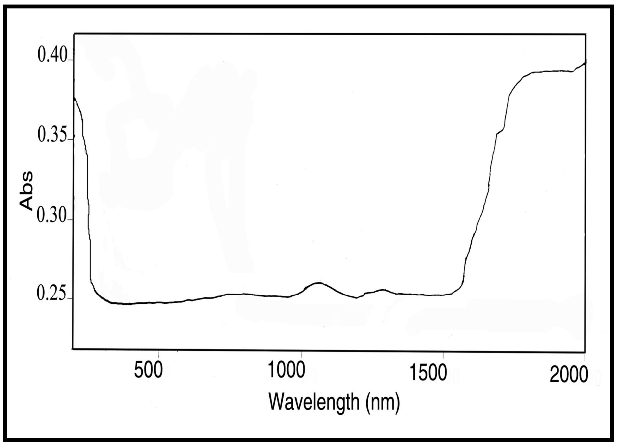

Fig. 4. Optical absorption spectrum of LPAN

3.6. Thermal Analysis

The thermogravimetric and differential thermal analysis of L-Phenylalanine L-phenylalaninium nitrate (LPAN) was carried out between 46 and 485°C in nitrogen atmosphere at a scanning rate of 10°C /min. The TGA and DTA traces are shown in Fig.5.Two major weight losses starting at about 168 °C is observed from the TGA trace. The decomposition completes at about 424 °C leaving no residue. But below 168 °C, there is no weight loss, hence the crystal is completely free of any entrapped or physically adsorbed water. The resulting DTA trace is a weak exotherm starting at about 169 °C which may be assigned to isomorphic transformation, as there is no corresponding weight loss in the TGA trace. This exothermic transition is followed by an intense small endotherm. It is matching with the intense weight loss in TGA starting at 168°C. There are endotherm and exotherm between 168 and 240 °C due to the decomposition of the residue in two stages. The total weight loss of these two stages corresponds to 48% due to the decomposition of nitrate ions to NO_2. Hence from this study it can be said that the crystal can retain its texture upto 168°C. Since the compound undergoes isomorphic transformation at 168 °C its application is restricted upto 168 °C.

3.7. Dielectric study

Fig. 6 and 7 show the variation of dielectric constant and the dielectric loss of LPAN crystal as a function of frequency at different temperatures (308, 328, 348, and 368 K). In the case of LPAN (Fig. 6), the dielectric constant is found to be 350.94 at 50 Hz and it decreases to 115.54 at 5 MHz. The variation in the value of ε_r is marginal in the frequency range 1 kHz-5 MHz. In addition, both the dielectric constant and dielectric loss increase with temperature. The very high value of ε_r at lower frequencies may be due to the space charge polarization. It is evident from Fig. 7. that the crystal has a very low dielectric loss in the high frequency region, which indicates the lesser number of defects in the crystal.

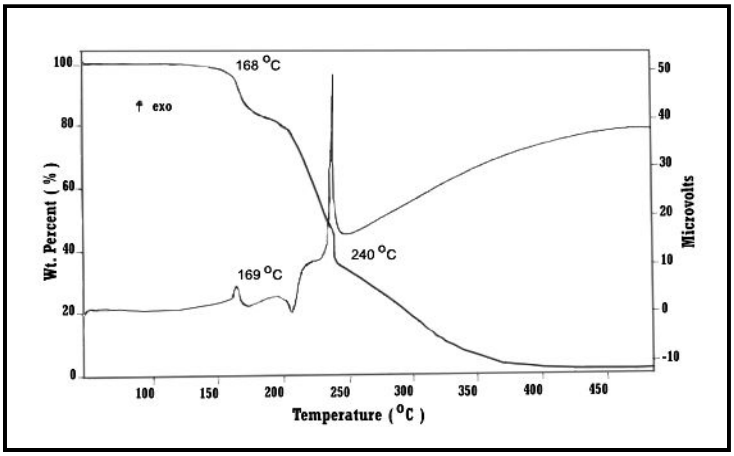

Fig. 5. TGA-DTA curve of LPAN

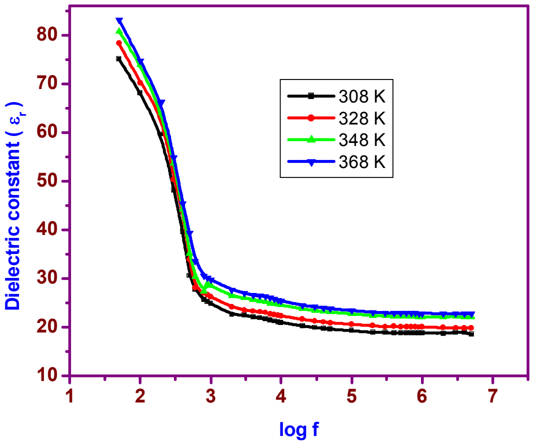

Fig. 6.Variation of dielectric constant with log frequency at different temperatures

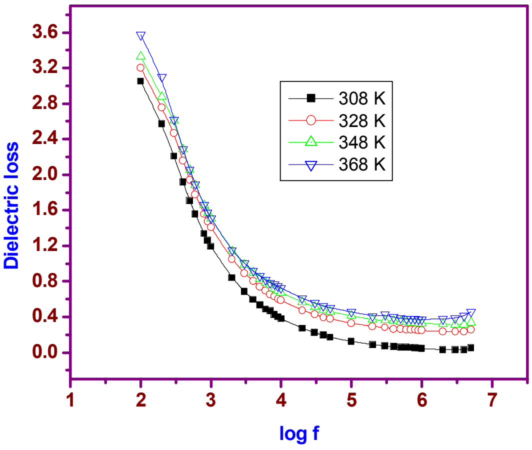

Fig. 7.Variation of Dielectric losses with log frequency at different temperatures

3.8. AC conductivity study

Fig. 8.shows the variation of *ac* conductivity (σ_{ac}) with temperature. At higher temperature, the increased conductivity could be due to the reduction in the space charge polarization. The conductivity of LPAN increases with increase in temperature. The electrical conduction is mainly a defect controlled process in low temperature region. It is observed from Fig.8. that the electrical conduction of LPAN is low at low temperature owing to trapping of some carriers at defect sites. As temperature rises, more and more defects are created, and as a result, the conductivity increases, which is predominantly due to moment of defects produced by thermal activation. Activation energy was found to be 0.043 eV from the plot (Fig. 9.).

3.9. DC conductivity study

Evaluation of *dc* electrical conductivity reveals useful information on the materials to exploit them for various applications. The study of *dc* electrical conductivity sheds light on the behaviour of charge carriers under a *dc* field, their mobility and mechanism of conduction. At any particular temperature, the Gibb's free energy of a crystal is minimum when a certain fraction of ions leave the normal lattice. As the temperature rises, more and more defects are produced which in turn, increases the conductivity. The dc conductivity of the crystal in the higher temperature region is determined by intrinsic defects caused by thermal fluctuations in the LPAN crystal (Fig. 10 and 11). Activation energy (E_{dc}) was also determined and it was found to be 0.042 eV.

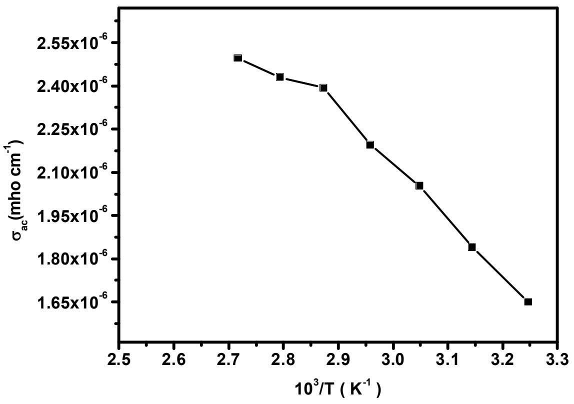

Fig. 8. Variation of ac conductivity with 1000/T for LPAN single crystal

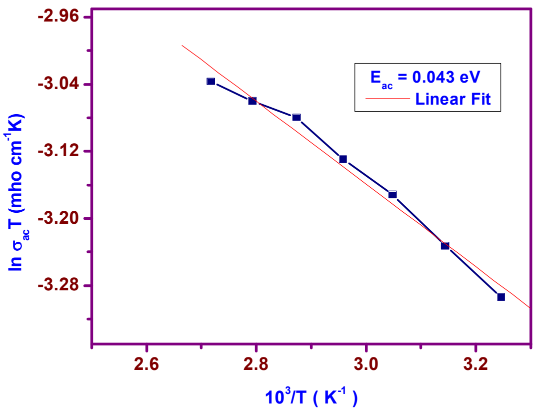

Fig. 9. Plot of ln(σ_{ac})T versus 1000/T for LPAN single crystal

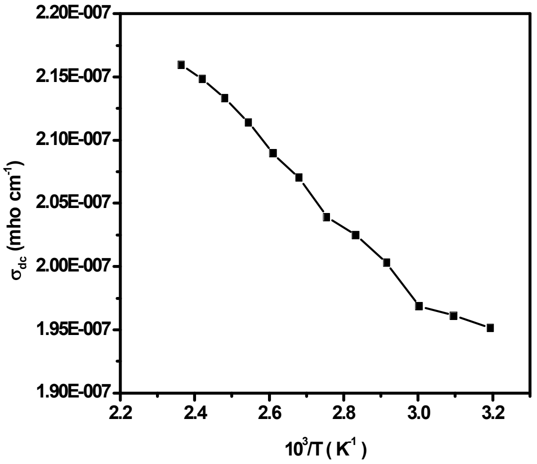

Fig. 10. Variation of dc conductivity with 1000/T for LPAN single crystal

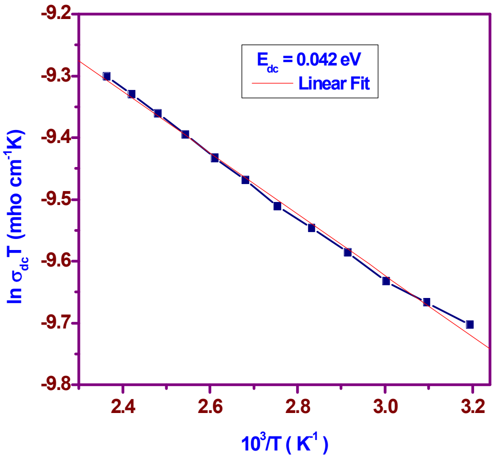

Fig. 11. Plot of ln(σ_{dc})T versus 1000/T for LPAN single crystal

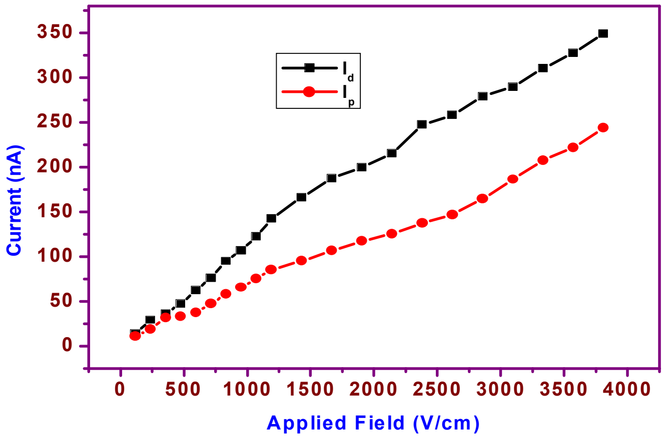

Fig. 12. Field dependent photoconductivity of LPAN single crystal

3.10. Photoconductivity study

Photoconductivity measurements were made using Keithley 485 picoammeter. The dark current was recorded by keeping the sample unexposed to any radiation. Fig. 12. shows the variation of both dark current (I_d) and photocurrent (I_p) with applied field. It is seen from the plots that both I_d and I_p of the sample increase linearly with applied field. It is observed from the plot that the dark current is always higher than the photo current, thus confirming the negative photoconductivity.

4. Conclusions

Single crystals of LPAN are conveniently grown by slow solvent evaporation technique. It is estimated from the X-ray diffraction studies that LPAN crystals are monoclinic and belong to $P2_1$ space group. The UV-Vis-NIR spectrum reveals the wider transmission window of LPAN and a low cut-off wavelength of 300 nm. The thermal studies prove that LPAN is thermally stable up to 168°C. The low dielectric loss with high efficiency implied that the sample possesses good optical quality with lesser defects. The photoconductivity investigations reveal the negative photo conducting nature of the sample. The activation energy is determined from the plots of *ac/dc* conductivity.

References

1. Ashley.D.V, Barclay.D.V, Chauffard. F.A, Moennoz. D, Leathwood P.D, Plasma amino acid responses in humans to evening meals of differing nutritional composition, Am. J. Clin. Nutr., 1982, 36 ,143-153.

2.Mahalakshmi.R, Jesuraja.S.X, Jerome Das.S, Growth and characterization of L-phenylalanine, Cryst. Res. Technol., 2006, 41,780-783.

3.Cao.X, Fischer.G, The infrared spectra and molecular structure of zwitterionic L-β-phenylalanine, J. Mol. Struct., 2006, 519,153-163.

4. Stewart.S, Fredericks.P.M, Surface-enhanced Raman spectroscopy of peptides and proteins adsorbed on an electrochemically prepared silver surface, Spectrochim. Acta. 1999, 55, 1615-1640.

5. Stephen P. A. Fodor, Robert A. Copeland, Christine A. Grygon, Thomas G. Spiro., Deep-ultraviolet Raman excitation profiles and vibronic scattering mechanisms of phenylalanine, tyrosine, and tryptophan, J. Am. Chem.Soc., 1989, 111, 5509-5518.

6.Costa Pessoa.J, Cavaco.I, Correia.I, Duarte.M.T, Gillard.R.D, Henriques.R.T,Higes.F.J, Madeira.C, Tomaz.T,Preparation and characterisation of new oxovanadium(IV) Schiff base complexes derived from amino acids and aromatic *o*-hydroxyaldehydes, Inorg. Chim. Acta,1999, 293, 1-11.

7. Ota.F, Higuchi.S, Gohshi.Y, Furuya.K, Ban.M, Kyoto.M, Some considerations of the SERS effect of L-phenylalanine in the near-infrared region using silver colloid solution, J. Raman Spectrosc., 1997, 28,849-854.

8. Al.karaghouli.A.R, Koezle.T.F, Neutron diffraction study of L-phenylalanine hydrochloride, Acta Cryst. B, 1975, 31, 2461-2465.

9. Nagashima, Chiaki Sano, Tetsuya Kawakita and Yoichi Iitaka, The crystal structure of Di-L-

Phenylalanine sulfate Monohydrate, Analytical Sciences, 1992, 8, 723-725.

10. Srinivasan.N and Rajaram. R. K, L-Phenylalanine L-Phenylalaninium Perchlorate, Acta Cryst. C, 1997, 53, 1711-1713.

11. Srinivasan.N, Sridhar.B, Rajaram. R.K., L-Phenylalanine–nitric acid (2/1), ActaCryst.E, 2001, 57, o916-o918.

12. Kalaiselvi.D, Mohan Kumar.R, Jayavel.R, Growth and Characterization of nonlinear optical L-arginine maleate dehydrate single crystals, Materials Letters, 2008, 61, 755-758.

*****